PREDICTION OF DAMAGE DUE TO COMPACTION DURING MANUFACTURING OF TEXTILE COMPOSITES

M.S. Islam[1], P. Prabhakar*[1], H. Kreiger[2], S. Stapleton[2], T. Gries[2]

[1] *Department of Mechanical Engineering, University of Texas at El Paso, TX*
[2] *Institute for Textiles, RWTH-Aachen, Aachen, Germany*
* *Corresponding Author: pprabhakar@utep.edu*

Keywords: keyword1 Textile Composite keyword2 Manufacturing keyword3 Computational Modeling keyword4 Damage

Abstract

The influence of fiber tows on the deformation and damage evolution in fiber reinforced composites is investigated by considering a micromechanical model of fibers within matrix that is undergoing compaction and subsequently subjected to mechanical loads. The stresses developed due to compaction of the matrix during the VARTM manufacturing process is modeled using the finite element (FE) framework. Nonlinear material behavior due to post-damage response that can lead to cracking in the matrix is incorporated through a crack band model that preserves mesh objectivity in the FE calculations. The mechanical response of the composite along with damaging capability due to compaction and subsequent mechanical loading is investigated in detail in this paper. The influence of the curing process is not considered in this paper. But, the final quality of the composite, subjected to varying compaction, is investigated using a mesoscale model.

1. Introduction

Textile composites are finding extensive use in the aerospace and automobile industry due to their high stiffness to volume ratio, easy formability and drapability[1]. For a rapid development of these materials in terms of high strength and durability, there is a need for a thorough understanding of the material state, and the influence of processing on the material response in subsequent service applications. Therefore, along with design aspects, like geometrical design and weaving, manufacturing induced defects have to be accounted for. These defects act as global failure initiation points within the composite. Therefore, in order to minimize any premature failure in the final composite manufactured, it is crucial to investigate process induced defect in these composites.

The most commonly used manufacturing technique for textile composites is the Vacuum Assisted Resin Transfer Molding (VARTM). In this technique, layers of dry fabric of the textile are place on top of each other, and subjected to vacuum. Further, liquid resin is transferred through the dry fabric through injection tubes, and is subjected to pressure and temperature as a curing process to manufacture the composite. The effects of compaction before or during the resin infusion are that the yarn has a very complicated shape and the fiber volume fractions vary

locally[[2], [3]]. Nesting occurs between the yarns [[2],[4],[5]] . Further, compaction creates complicated contact zones between the yarns [[1]-[3]]. Grail et al.[6] developed a new finite element mesh generation method for textile preform and compacted reinforcement.

The inputs to the manufacturing process influence the outcome of the composite in different ways. The pressure applied to the dry fabric, the rate of resin injection, the temperature during curing, are a few processes that may alter the quality of the final laminate. Therefore, it will be useful to the industry, if there are computational tools which are able to predict the final outcome of the VARTM process.

In this paper, the influence of the compaction on woven glass fabric during the VARTM process is investigated. In this context, the tensile response of the woven composite subjected to varying compaction is computationally studied. As a first approach, compaction on fabric layer during manufacturing and tension on the final composite was considered in this paper. Stresses developed during the curing process of resin is not considered in this paper which is under consideration as a next step.

Mesoscale models of 4 layers of the woven glass composite are considered. Section 3 describes the geometry and the material used in the representative volume element (RVE) of the composite. Further, in Section 4, the model for compaction is discussed, followed by tensile loading response of the compacted model. Damage and failure of the matrix between the tows is modeled to account for the effect of compaction. A parametric study of the matrix fracture properties is conducted to determine the tensile response of the composite.

2. Modeling Approach

The computational modeling approach is divided into two parts: 1) Compaction of the fiber tows with uncured resin, and 2) Tensile response of the post-cured composite with damaging capability included in the matrix.

3. Mesoscale Model

Four layers of glass fabric (as reinforcement) and Epon 638 with Epikure (as matrix) was used in the paper. Fig. 1 shows the RVE with woven fiber tows and matrix. Fig. 2(a) shows a single layer of glass fabric with an exaggerated view. A schematic of a single tow, with it's dimensions, used in the model is shown in Fig. 2(b). The in-plane spacing between two successive yarns is approximately 0.3 mm. Geometry of the RVE was modeled with TexGen software, which is specially designed to model textile composites. The geometry of the model was then exported to ABAQUS (a commercially available software) to perform the finite element analysis.

4. Computational Modeling of Compaction

In the compaction step, the RVE shown in Fig. 1 is used. The properties of the glass fiber used in this model are E_f= 85 GPa and ν_f=0.22. For the compaction model, it is assumed that the liquid resin fills the entire space between the dry fabric. Therefore, prior to solidification of the resin, it was considered that 5 % of the resin has already cured. The matrix properties at this stage are E_m=0.081 GPa and ν_m = 0.48 [7]. The homogenized tow properties were calculated

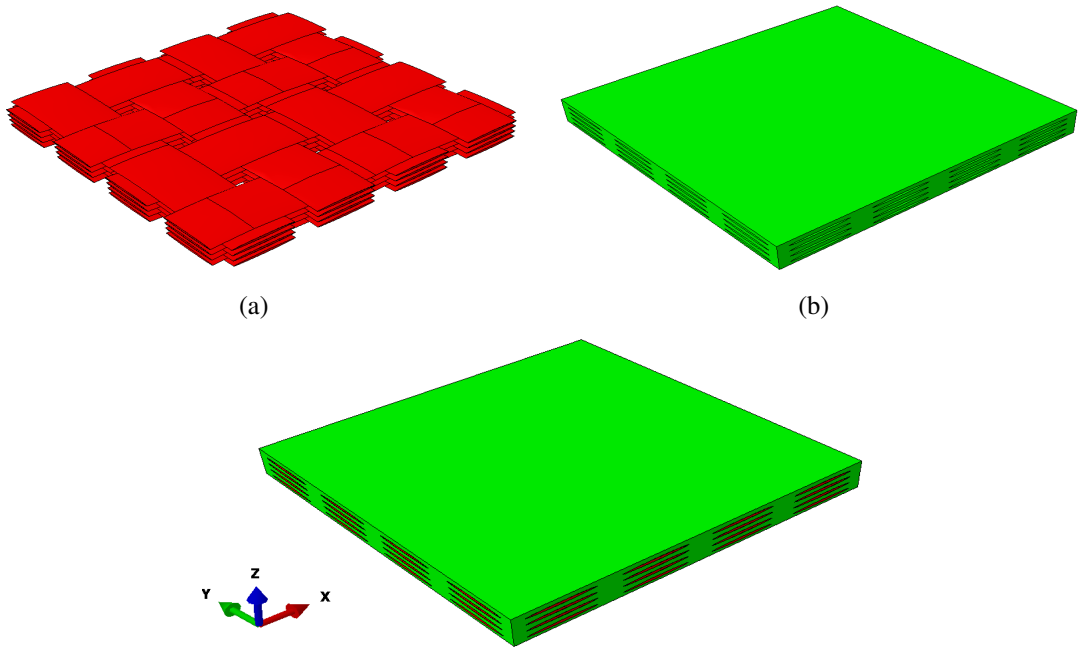

Figure 1. RVE of the Woven Composite

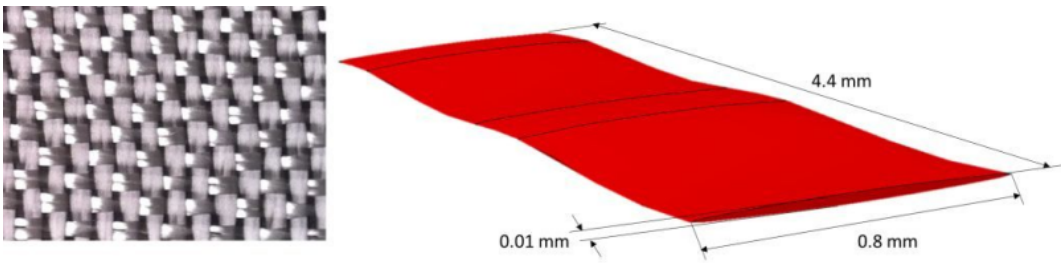

Figure 2. (a) Woven Glass Fabric and (b) Single Tow with Dimensions.

using these properties of fiber and matrix using the concentric cylinder model [8]. Table 1 shows the homogenized properties of tows in the uncured state.

The boundary conditions used in the compaction modeling are shown in Fig. 3(a). Displacement of the bottom surface was restricted in the z-direction, and a displacement condition simulating a compaction was applied on the top surface. All other faces were maintained to be flat, i.e. the faces all allowed to breathe while remaining flat. Five different compactions, i.e. 5%, 7.5%, 10%, 30% and 50% of the thickness of composite were considered to study the effect of compaction of the final composite.

Table 1. Homogenized Tow Properties with 5% cured Matrix

E_{11}(GPa)	E_{22}(GPa)	$\nu_{12} = \nu_{13}$	ν_{23}	$G_{12} = G_{13}$(GPa)	G_{12} (GPa)
51.034	0.254	0.307	0.2142	0.111	0.105

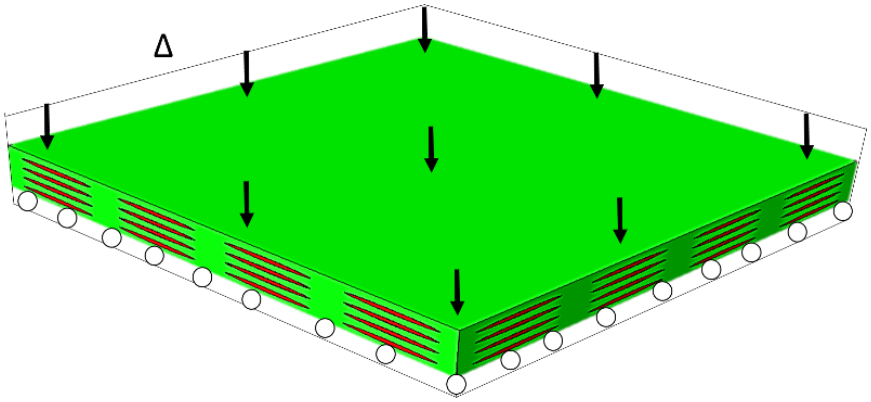

(a)

Figure 3. Boundary Conditions for Compaction Modeling

5. Tensile Modeling of the Compacted Composite

The models corresponding to the different compaction values are subjected to tensile loading post-cure. As mentioned above, the curing process is not modeled in this paper. Therefore, the cured matrix properties were considered for the tensile loading step. That is, the cured matrix properties are E_m=4.95 GPa and ν_m=0.375 [7]. Table 2 shows the corresponding homogenized tow properties. Boundary conditions for this case is shown in Fig. 4(a). Flat boundary conditions mentioned used for the compaction step was used for free surfaces in this current step as well.

Table 2. Homogenized Tow Properties of Final Composite

E_{11}(GPa)	E_{22}(GPa)	$\nu_{12} = \nu_{13}$	ν_{23}	$G_{12} = G_{13}$(GPa)	G_{12} (GPa)
53.01	13.67	0.375	0.251	6.044	5.468

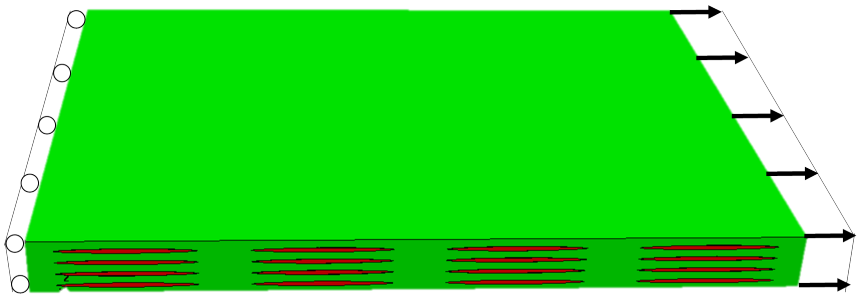

(a)

Figure 4. Boundary Conditions for Tension Modeling

5.1. Damage Capability in Matrix: Crack Band Model

Crack Band theory (CBM) [9] was implemented into the matrix properties to introduce damage in the matrix. This theory was introduced in the model by means of a user subroutine compatible with ABAQUS. Only damage in the matrix was considered in this study.

The inputs to the CBM are the cohesive law for the matrix. Fracture toughness (G_c) and critical strengths (σ_c) are the two inputs to the cohesive law. The cured matrix behaves like a linear isotropic material until the critical strength, beyond which it starts to degrade. The matrix is completely failed when the entire fracture toughness is exhausted during the fracture process. Due to the presence of a negative tangent stiffness in the constitutive law due to the fracture process, it renders the finite element method (FEM) model pathologically mesh dependent. The CBM scales the energy dissipated with the element size in the FEM model, making the model mesh objective.

6. Results and Discussions

For the compaction modeling, 5 different displacements for compaction were used, i.e., 5%, 7.5%, 10%, 30% and 50% of the thickness of the composite (in the z-direction). Table 3 shows the original and deformed dimensions because of compaction. Here, the original length of the RVE is $L = 4.4mm$, and the thickness $t = 0.44mm$, the corresponding dimensions after different compaction are given in the table.

Table 3. Original and Deformed Dimensions after Compaction

Model	L (mm)	t (mm)
Original	4.4	0.44
5 % Compaction	4.40564	0.418
7.5 % Compaction	4.40846	0.407
10 % Compaction	4.41128	0.396
30 % Compaction	4.43383	0.308
50 % Compaction	4.45638	0.22

Fig. 5 shows the load-displacement diagrams for tensile response for different compaction and varying critical stress values (σ_c) for the matrix. The initial stiffness for 5%, 7.5% and 10% compaction is almost same for all values of , but this stiffness reduced because of more compaction (30% or 50% compaction). So, the amount of compaction plays an important role on the initial stiffness of the final composite. Fig. 5 also shows that the global tensile failure load decreases with increase in compaction.

The tensile load corresponding to first damage initiation in the composite is plotted in Fig. 6(a) for varying compaction and σ_c values. It is observed that the loads reduce with increasing compaction and reducing σ_c. Similar behavior is observed for tensile loads at first failure points for different compaction and varying σ_c in Fig. 6(b). Fig. 6(a) and Fig. 6(b) indicate that when the compaction is increased from 5% to 50%, the loads for damage initiation reduces by 50%, and for the first failure point reduces by approximately 43%. For illustration, the damaged and the failed regions in the composite for 5% compaction and $\sigma_c = 45MPa$, are shown in red in Fig. 7(a) and Fig. 7(b). This indicates that the composite with greater compaction during manufacturing will fail prematurely when subjected to service loads.

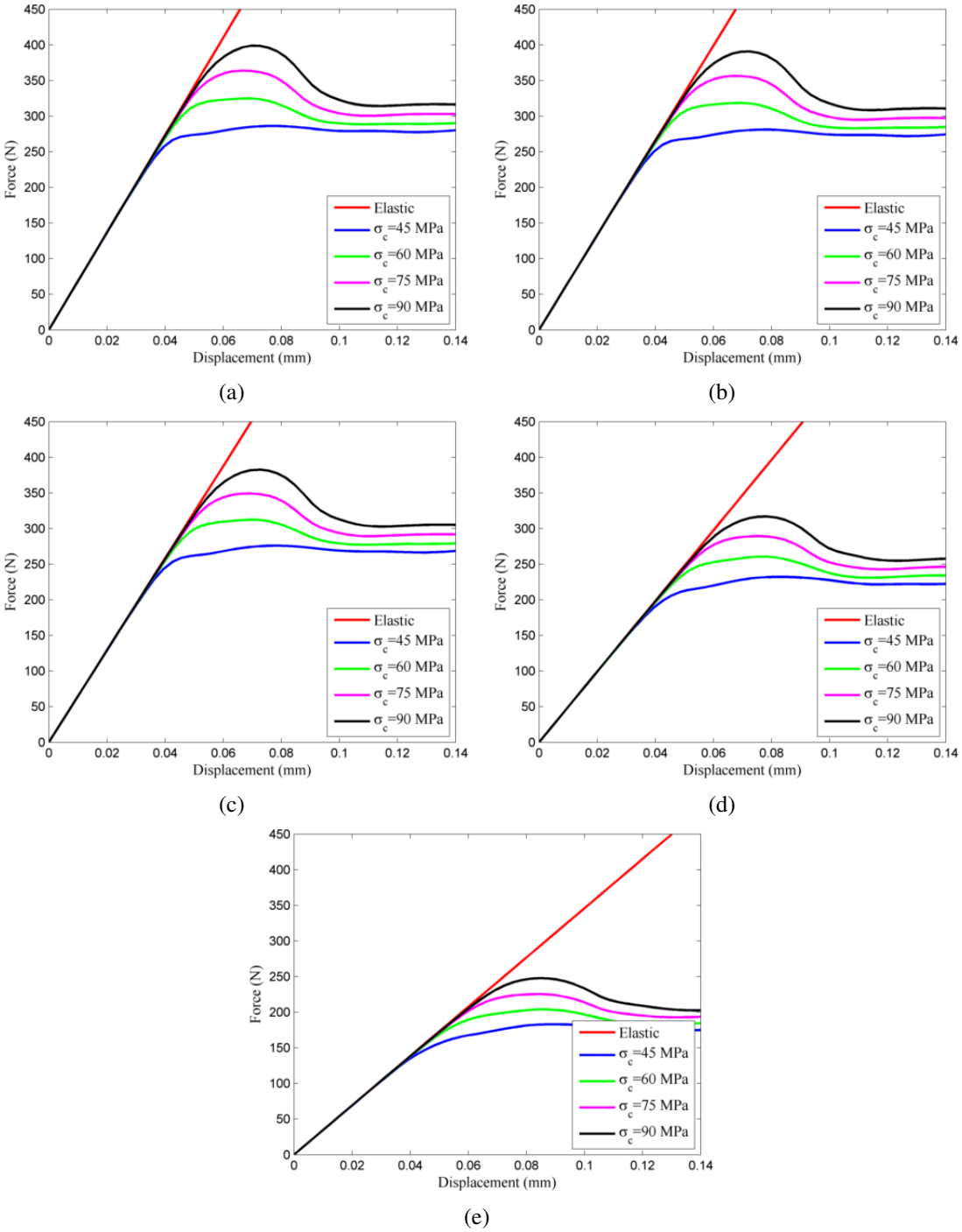

Figure 5. Load Displacement Response corresponding to Varying σ_c at Different Compactions of (a) 5%, (b) 7.5%, (c) 10%, (d) 30%, and (e) 50%

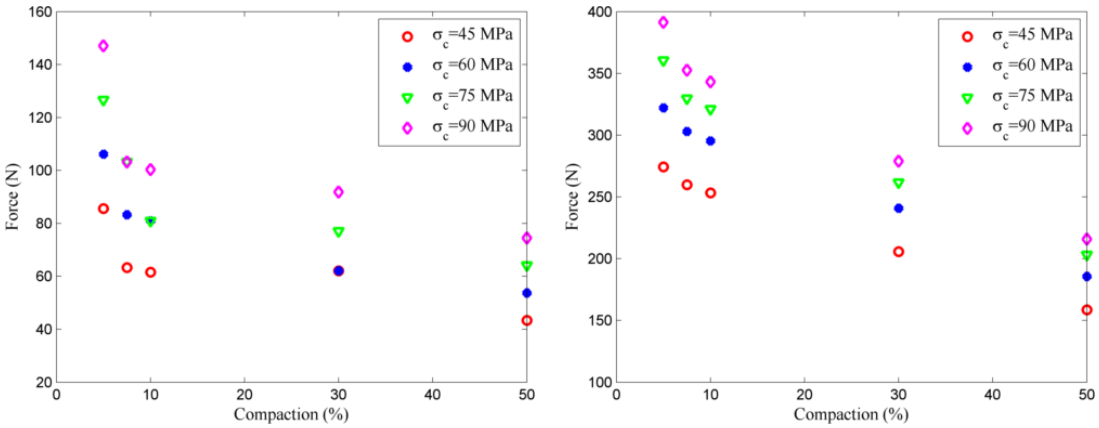

Figure 6. Loads at (a) First Damage and (b) Failure Points

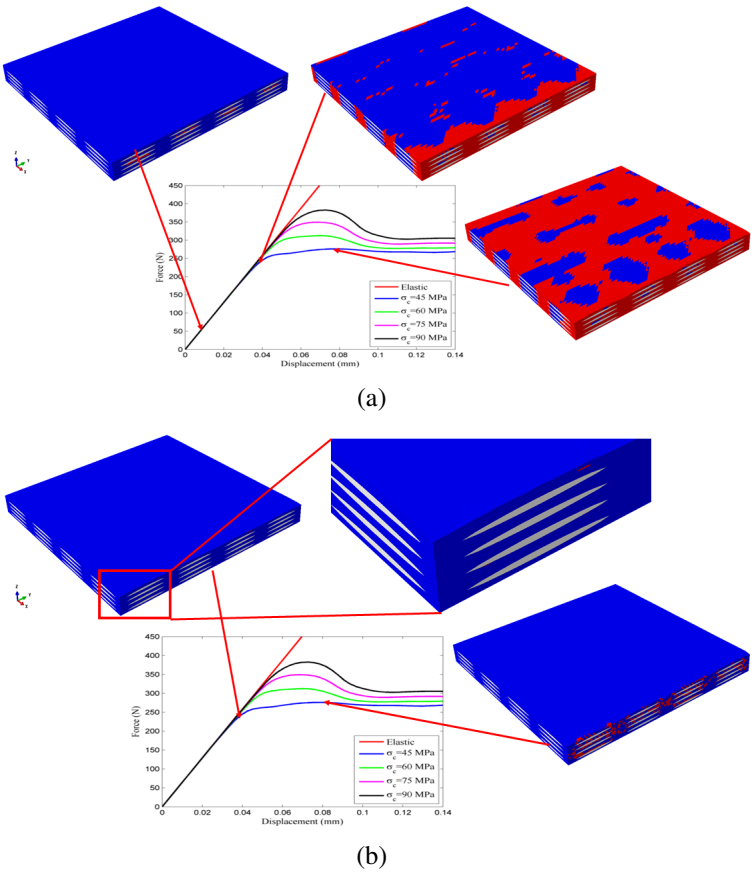

Figure 7. Example of Damaged and Failed Regions; Compaction = 5% and $\sigma_c = 45MPa$

References

[1] A.P. Mouritz, M.K. Bannister, P.J. Falzon, and K.H. Leong. Review of applications for advanced three-dimensional fibre textile composites. *Composites Part A: Applied Science and Manufacturing*, 30(12):1445–1461, 1999. doi: http://dx.doi.org/10.1016/S1359-835X(99)00034-2.

[2] M. Olave, A. Vanaerschot, S.V. Lomov, and D. Vandepitte. Internal geometry variability of two woven composites and related variability of the stiffness. *Polymer Composites*, 33(8):1335–1350, 2012. URL `http://dx.doi.org/10.1002/pc.22260`.

[3] M. Karahan, S.V. Lomov, A.E. Bogdanovich, D. Mungalov, and I. Verpoest. Internal geometry evaluation of non-crimp 3d orthogonal woven carbon fabric composite. *Composites Part A: Applied Science and Manufacturing*, 41(9):1301 – 1311, 2010. doi: http://dx.doi.org/10.1016/j.compositesa.2010.05.014.

[4] B. Chen, E.J. Lang, and T-.W. Chou. Experimental and theoretical studies of fabric compaction behavior in resin transfer molding. *Materials Science and Engineering: A*, 317(12):188 – 196, 2001. doi: http://dx.doi.org/10.1016/S0921-5093(01)01175-3.

[5] S.V. Lomov, I. Verpoest, T. Peeters, D. Roose, and M. Zako. Nesting in textile laminates: geometrical modelling of the laminate. *Composites Science and Technology*, 63(7):993 – 1007, 2003. doi: http://dx.doi.org/10.1016/S0266-3538(02)00318-4.

[6] G. Grail, M. Hirsekorn, A. Wendling, G. Hivet, and R. Hambli. Consistent finite element mesh generation for meso-scale modeling of textile composites with preformed and compacted reinforcements. *Composites Part A: Applied Science and Manufacturing*, 55(0):143 – 151, 2013. doi: http://dx.doi.org/10.1016/j.compositesa.2013.09.001.

[7] C. Heinrich, M. Aldridge, A.S. Wineman, J. Kieffer, A.M. Waas, and K.W. Shahwan. Generation of heat and stress during the cure of polymers used in fiber composites. *International Journal of Engineering Science*, 53 (0):85 – 111, 2012. doi: http://dx.doi.org/10.1016/j.ijengsci.2011.12.004.

[8] M. Hyer and A.M. Waas. Micromechanics of linear elastic continuous fiber composites. *Comprehensive composite materials*, 1:345–375, 2000.

[9] Z. Bazant and B.H. Oh. Crack band theory for fracture of concrete. *Matriaux et Construction*, 16(3):155–177, 1983. doi: 10.1007/BF02486267.